



A bromine explosion event linked to cyclone development in the Arctic

A.-M. Blechschmidt et al.

This discussion paper is/has been under review for the journal Atmospheric Chemistry and Physics (ACP). Please refer to the corresponding final paper in ACP if available.

An exemplary case of a bromine explosion event linked to cyclone development in the Arctic

A.-M. Blechschmidt¹, A. Richter¹, J. P. Burrows¹, L. Kaleschke², K. Strong³, N. Theys⁴, M. Weber¹, X. Zhao³, and A. Zien^{1,a}

¹Institute of Environmental Physics, University of Bremen, Bremen, Germany

²Institute of Oceanography, University of Hamburg, Hamburg, Germany

³Department of Physics, University of Toronto, Toronto, Ontario, Canada

⁴Belgian Institute for Space Aeronomy (IASB-BIRA), Brussels, Belgium

^anow at: Energy and Meteo Systems GmbH, Oldenburg, Germany

Received: 16 July 2015 – Accepted: 14 August 2015 – Published: 15 September 2015

Correspondence to: A.-M. Blechschmidt (anne.blechschmidt@iup.physik.uni-bremen.de)

Published by Copernicus Publications on behalf of the European Geosciences Union.

Title Page

Abstract

Introduction

Conclusions

References

Tables

Figures



Back

Close

Full Screen / Esc

Printer-friendly Version

Interactive Discussion



Abstract

Intense, cyclone-like shaped plumes of tropospheric bromine monoxide (BrO) are regularly observed by GOME-2 on board the MetOp-A satellite over Arctic sea ice in polar spring. These plumes are often transported by high latitude cyclones, sometimes over several days despite the short atmospheric lifetime of BrO. However, only few studies have focused on the role of polar weather systems in the development, duration and transport of tropospheric BrO plumes during bromine explosion events. The latter are caused by an autocatalytic chemical chain reaction associated with tropospheric ozone depletion and initiated by the release of bromine from cold brine covered ice or snow to the atmosphere.

In this manuscript, a case study investigating a comma-shaped BrO plume which developed over the Beaufort Sea and was observed by GOME-2 for several days is presented. By making combined use of satellite data and numerical models, it is shown that the occurrence of the plume was closely linked to frontal lifting in a polar cyclone and that it most likely resided in the lowest 3 km of the troposphere. In contrast to previous case studies, we demonstrate that the dry conveyor belt, a potentially bromine-rich stratospheric air stream which can complicate interpretation of satellite retrieved tropospheric BrO, is spatially separated from the observed BrO plume. It is concluded that weather conditions associated with the polar cyclone favored the bromine activation cycle and blowing snow production, which may have acted as a bromine source during the bromine explosion event.

1 Introduction

Intense plumes of bromine monoxide (BrO) are regularly observed over sea ice during polar spring by satellite (e.g. Richter et al., 1998; Wagner and Platt, 1998; Hollwedel et al., 2004; Choi et al., 2012; Theys et al., 2011; Sihler et al., 2012) and ground-based instruments (e.g. Frieß et al., 2004, 2011; Nghiem et al., 2012). Although subsidence

ACPD

15, 24955–24993, 2015

A bromine explosion event linked to cyclone development in the Arctic

A.-M. Blechschmidt et al.

Title Page

Abstract

Introduction

Conclusions

References

Tables

Figures



Back

Close

Full Screen / Esc

Printer-friendly Version

Interactive Discussion



A bromine explosion event linked to cyclone development in the Arctic

A.-M. Blechschmidt et al.

Title Page

Abstract

Introduction

Conclusions

References

Tables

Figures

⏪

⏩

◀

▶

Back

Close

Full Screen / Esc

Printer-friendly Version

Interactive Discussion



of stratospheric air towards lower altitudes can substantially increase total column BrO (Salawitch et al., 2010), several studies have shown that the plumes are often of tropospheric origin and occur in conjunction with widespread ozone depletion (Barrie et al., 1988; Simpson et al., 2007b; Jones et al., 2013). The latter is caused by an autocatalytic, heterogeneous chemical cycle, the so called “bromine explosion” (Barrie and Platt, 1997; Lehrer et al., 1997; Platt and Lehrer, 1997), in which gas phase molecular bromine is photolysed in the presence of sunlight and oxidised subsequently by ozone to form BrO. The latter then reacts with HO₂ to form HOBr which is eventually removed from the atmosphere by wet scavenging. The exact chemical reaction cycle as well as the substrate, from which bromine is initially released to the gas phase are still unclear (Jones et al., 2009). However, there is general agreement that the source must be rich in sea salts and specifically in Br⁻ which reacts within the condensed phase substrate to form Br₂ which is released to the atmosphere:



It is important to note that a pH lower than 6.5 is required for an efficient bromine activation cycle (Fickert et al., 1999). The possible sequence of reactions involved in the bromine explosion is given in detail in numerous studies (e.g. Sander et al., 2006; Simpson et al., 2007b; Buys et al., 2013).

According to Rankin et al. (2002), frost flowers are a primary source of bromine involved in ozone depletion due to their large surface areas and salinities of about three times higher than in sea water. Kaleschke et al. (2004) combined sea ice coverage and tropospheric BrO from satellite remote sensors with regions potentially covered by frost flowers derived from a simple thermodynamic model. This was based on noting cold surface temperature and related conditions associated with source regions for

A bromine explosion event linked to cyclone development in the Arctic

A.-M. Blechschmidt et al.

Title Page

Abstract

Introduction

Conclusions

References

Tables

Figures



Back

Close

Full Screen / Esc

Printer-friendly Version

Interactive Discussion



BrO. They concluded that young ice regions covered by frost flowers are the source of bromine in bromine explosion events (termed BEEs in the following). Domine et al. (2005) stated that the role of frost flowers for heterogeneous reactions should be re-considered, as they measured the total surface area of frost flowers in the Arctic to be only $1.4 \text{ m}^2 \text{ m}^{-2}$ of ice surface. Roscoe et al. (2011) investigated frost flowers in the lab and could not observe release of aerosols despite wind speeds in gusts up to 12 m s^{-1} . Correlating BrO measurements with air mass histories from meteorological back trajectories, Simpson et al. (2007a) identified snow and ice contaminated with sea salt on first-year sea ice as a more likely bromine source compared to frost flowers at Barrow in Alaska. However, results by Obbard et al. (2009) suggest that blowing snow could be salinated by frost flower contact and that, as a consequence, frost flowers and blowing snow in combination are the major source of atmospheric bromine.

Yang et al. (2010) found a good agreement with satellite derived tropospheric BrO when including sublimation of salty blowing snow as a bromine source in a chemical transport model. Pratt et al. (2013) conducted snow chamber experiments on various types of snow and ice surfaces at Barrow, Alaska, and concluded that photochemical production of molecular bromine in surface snow may serve as a major bromine source. They found the most effective production rates of Br_2 for tundra snow and the uppermost 1 cm thick layer of snow on top of first-year sea ice. Using GOME satellite data, Wagner et al. (2001) linked the development of boundary layer BrO plumes to locations of 1 year old sea ice.

Younger sea ice has gained much attention in studies on BEEs as it is much more salty than older ice (Nghiem et al., 2012) so that snow lying on this ice can easily accumulate sea-salt (Yang et al., 2010). Moreover, liquid brine which forms on fresh ice during the freezing process is highly concentrated in sea-salts. Frost flowers growing on the ice or snow lying on top of it can get coated with the brine through capillary forces (Sander et al., 2006). The likeliness for production of atmospheric Br_2 through heterogeneous reaction is enhanced, if the frost flowers, salty snow or sea salt aerosols are lifted up into the air by high wind speeds as will be described below. Nghiem et al.

fect of multiple scattering between surface and cloud bottom which enhances the light path below the cloud, partly compensating for the smaller number of photons which penetrate the cloud. The influence of clouds on box airmass factors does not vary much for solar zenith angles between 60 and 80°, which is characteristic for the BCTE observations discussed in this paper.

Further investigation of GOME-2 O₄ retrievals (not shown) indicate that light path enhancement due to multiple scattering caused by clouds cannot explain the large VCDs observed inside the BrO plume for the case investigated in the present study. This agrees with the box airmass factor displayed in Fig. 1, which only shows a rather small increase in the upper parts of clouds compared to the cloud free case, even for a cloud optical thickness of 100.

GOME-2 total columns of ozone derived using the Weighting Function DOAS (WF-DOAS) (Coldewey-Egbers et al., 2005; Weber et al., 2005; Bracher et al., 2005) are incorporated in the present study to better differentiate between stratospheric and tropospheric air flows within the polar cyclone.

2.2 MODIS

The Moderate Resolution Imaging Spectroradiometer (MODIS) on board the National Aeronautics and Space Administration (NASA) Terra and Aqua satellites measures visible and thermal electromagnetic radiation in 36 spectral bands between 0.4 and 14.4 µm (<http://modis.gsfc.nasa.gov>). In this manuscript, false colour images are constructed using the 2.1 µm mid-infrared channel for both red and green and the 0.85 µm visible channel as blue following the blowing snow detection method by Palm et al. (2011). For such imaging, snow and ice on the ground should appear blue, as their signal stands out in the visible, while clouds and suspended snow particles should appear yellow, as these cause signals which stand out in the mid-infrared (Palm et al., 2011). MODIS false colour images are used here to investigate if blowing snow may have contributed as a bromine source during the BCTE and, in combination with GOME-2 ozone observations, to distinguish between stratospheric and tropospheric air flows.

A bromine explosion event linked to cyclone development in the Arctic

A.-M. Blechschmidt et al.

Title Page

Abstract

Introduction

Conclusions

References

Tables

Figures



Back

Close

Full Screen / Esc

Printer-friendly Version

Interactive Discussion



The MODIS data with 1 km horizontal resolution is provided by NASA through the MODIS website (<http://modis.gsfc.nasa.gov>).

2.3 SMOS

5 The Microwave Imaging Radiometer with Aperture Synthesis (MIRAS) on board the Soil Moisture and Ocean Salinity (SMOS) satellite measures radiance emitted by the Earth at L-Band (1.4 GHz). MIRAS has a footprint of 35 km in nadir, while the footprint is 45 km at the edges of the swath (Kaleschke et al., 2012). An iterative retrieval algorithm was used to calculate sea ice thickness from the 1.4 GHz near nadir brightness temperature (Tian-Kunze et al., 2014). SMOS sea ice thickness maps are indicative
10 of conditions for sea ice surfaces with high salinity because the 1.4 GHz brightness temperature is in particular sensitive to thin ice and leads in sea ice.

2.4 CALIOP

15 The Cloud Aerosol Lidar with Orthogonal Polarization (CALIOP) on board the Cloud-Aerosol Lidar Infrared Pathfinder Satellite Observation (CALIPSO) satellite is a two-wavelength polarization-sensitive lidar which provides high-resolution vertical profiles of clouds and aerosols (<http://www-calipso.larc.nasa.gov>). As it is difficult to obtain cloud information from passive remote sensors over snow or sea ice, CALIOP is used to investigate cloud top altitudes inside the BCTE. CALIOP data were obtained from the NASA Langley Research Center Atmospheric Science Data Center through their
20 website at <http://eosweb.larc.nasa.gov/>.

A bromine explosion event linked to cyclone development in the Arctic

A.-M. Blechschmidt et al.

Title Page

Abstract

Introduction

Conclusions

References

Tables

Figures



Back

Close

Full Screen / Esc

Printer-friendly Version

Interactive Discussion



3 Numerical model simulations

3.1 WRF

The WRF model is a mesoscale numerical weather prediction and atmospheric simulation system developed at the National Center for Atmospheric Research (NCAR) (Skamarock et al., 2008).

Here, we use WRF version 3.6 to simulate meteorological conditions for a 7600 km × 7600 km sized domain centred on the development region of the BCTE (see Fig. 2 for the borders of the model domain). The model is run with a horizontal grid spacing of 20 km × 20 km, 30 levels in the vertical and a model top at 50 hPa. NCEP Final Analysis (FNL from GFS) 6 hourly data with 1° resolution is used to initialise meteorological conditions and as boundary conditions. The NCEP FNL data was provided by the Computational and Information Systems Laboratory (CISL) Research Data Archive through their web site at <http://dss.ucar.edu/>. The simulation starts on 31 March 2011 at 00:00 UTC and ends on 3 April at 00:00 UTC. WRF output is produced at a half-hourly time step, so that the model output is close to satellite observation times.

Our model set-up includes the Mellor-Yamada-Janjic planetary boundary layer scheme (Janjic, 1994), Lin et al. (1983) for cloud microphysics, the Dudhia (1989) shortwave radiation scheme and the Rapid Radiative Transfer Model longwave radiation scheme (Mlawer et al., 1997).

3.2 FLEXPART

FLEXPART is a Lagrangian trajectory model suitable for simulating a large range of atmospheric transport processes (<http://www.flexpart.eu>). It has been used in atmospheric chemistry research to examine source regions for aircraft, satellite, ground-based station, and ship-based studies (Stohl et al., 2005; Stohl, 2006; Warneke et al., 2009; Begoin et al., 2010; Gilman et al., 2010; Hirdman et al., 2010).

ACPD

15, 24955–24993, 2015

A bromine explosion event linked to cyclone development in the Arctic

A.-M. Blechschmidt et al.

Title Page

Abstract

Introduction

Conclusions

References

Tables

Figures



Back

Close

Full Screen / Esc

Printer-friendly Version

Interactive Discussion



A bromine explosion event linked to cyclone development in the Arctic

A.-M. Blechschmidt et al.

[Title Page](#)[Abstract](#)[Introduction](#)[Conclusions](#)[References](#)[Tables](#)[Figures](#)[Back](#)[Close](#)[Full Screen / Esc](#)[Printer-friendly Version](#)[Interactive Discussion](#)

In the present study, FLEXPART is run forward in time for a passive BrO tracer which is transported by winds from 1° resolution NCEP Final Analysis 6 hourly data. As knowledge of BrO chemistry is limited, simulations are kept as simple as possible, so that the BrO tracer is not removed by wet or dry deposition and no assumptions on its lifetime were made. Convection is accounted for in our model configuration. FLEXPART output is produced half-hourly (as for WRF, see Sect. 3.1) on a 1° resolution grid.

FLEXPART runs are initialised by daily averaged GOME-2 satellite retrievals of tropospheric BrO following the method of Begoin et al. (2010). To identify the most likely source regions of tropospheric BrO for this event, which we expect to be located in close proximity of the plume, only satellite data with values above 5×10^{13} molec cm⁻² and between 140 to 280° E, to the north of 65° N are regarded here.

Results from three different sets of simulations will be shown below. The first set of FLEXPART simulations (FS1) is started and initialised on 1 April at 00:00 UTC by daily averaged satellite observations from approximately 31 March at 22:00 UTC to 1 April at 01:00 UTC. Note that possible initialisation times are limited to the 6 hourly time resolution of NCEP Final Analysis data. As the BrO plume location is nearly stationary for all orbits included in this satellite mean, we expect possible effects resulting from time gaps between initialisation and satellite observation to be negligible. The second set of simulations (FS2) is started and initialised on 2 April at 00:00 UTC by satellite observations from 1 April at about 20:00 to 23:00 UTC. Again, the plume is to a good approximation stationary for all orbits included in the satellite mean for 1 April. The third set of simulations (FS3) use the same set up as FS2, but in addition to the latitude and longitude boundaries given above, only observations up to 76° N are regarded here.

Each set of FLEXPART experiments consists of six model runs assuming that the plume was located between 0–1, 1–3, 3–5, 5–7, 7–9 or 9–11 km at time of initialisation. This means that the higher elevation runs are initialised by plumes above the tropopause. As will be described in the following section, the FLEXPART runs show that the plume resided in the troposphere, confirming that GOME-2 observed a tropospheric feature.

under stable shallow boundary layer conditions, are described in detail by Zhao et al. (2015). Overall, the observed lifetime of the high wind speed BCTE is about four days according to GOME-2 observations, covering the onset (evening of 31 March), mature stage (evening of 1 April) and dissolving stage (evening of 2 April).

5 The BrO plume observed by GOME-2 is spatially correlated to low temperatures around 350 gpm (see Fig. 4d, the difference between geopotential heights and altitudes above ground is assumed to be negligible) simulated by WRF, although the relation is less clear during the development of the event compared to later stages. The correlation is also present at higher altitudes up to roughly 500 gpm during the development
10 stage and roughly 1000 gpm for the mature and dissolving stage of the BCTE. This is in agreement with the results by Sander et al. (2006) (see Sect. 1), who found that recycling of BrO on aerosol surfaces is most efficient at low temperatures.

Figure 5 shows sea ice thickness retrieved by SMOS for 1 April. This date is chosen as a proxy of sea ice thickness conditions for other days during the BCTE (potential
15 bromine sources deduced from SMOS images do not change significantly from late March to early April 2011). SMOS shows reduced sea ice thicknesses in the area around -170° E, 77.5° N and -158° E, 74° N. Comparing GOME-2 observations of the BrO plume to SMOS retrievals and considering wind directions simulated by WRF, we infer that the former identified region may have acted as a bromine emission source
20 during the onset of the BCTE, while the latter region may have been a source of bromine during the mature stage of the event.

To identify the location of the BrO plume with respect to cyclonic air flows, ozone VCDs [DU] from GOME-2 as well as MODIS false colour images close to GOME-2
25 observation times are shown in Fig. 3c and e, respectively. Note that further inspection of all MODIS observations of the BCTE available before and after each GOME-2 observation indicates that MODIS orbits shown in Fig. 3 are to a good approximation representative of cloud/blowing snow conditions at GOME-2 observation times. The dry conveyor belt is a low moisture, ozone-rich air stream within an extra-tropical cyclone, descending from the lower stratosphere towards tropospheric altitudes. On

A bromine explosion event linked to cyclone development in the Arctic

A.-M. Blechschmidt et al.

[Title Page](#)[Abstract](#)[Introduction](#)[Conclusions](#)[References](#)[Tables](#)[Figures](#)[Back](#)[Close](#)[Full Screen / Esc](#)[Printer-friendly Version](#)[Interactive Discussion](#)

the stripy features observed by MODIS (see above). A reduced sea ice thickness indicates younger and saltier sea ice. Snow lying on top of younger sea ice, is covered in brine and more salty itself. This possibly favored the bromine explosion chemical chain reaction together with weather conditions in the area of stripy features observed by MODIS.

Left panels in Fig. 7 show CALIOP vertical feature mask giving insight into vertical cloud and aerosol distributions inside the BrO plume for all development stages of the BCTE. CALIPSO footprints corresponding to these CALIOP observations are given by red and black dotted lines plotted on top of MODIS false colour images and GOME-2 tropospheric BrO VCDs in Fig. 3e and a, respectively. Again, further inspection of all MODIS observations of the BCTE available before and after each CALIOP observation indicates that MODIS observations shown in Fig. 3 are to a good approximation representative of cloud conditions at CALIOP observation times. Comparing the vertical feature masks with GOME-2 tropospheric BrO VCD along corresponding CALIPSO footprints (Fig. 7, right panels) shows that at the plume location, clouds and aerosols were restricted to about 3 km height in the vertical (with the exception of the onset of the event, for which some parts of the plume occurred in an area of higher cloud tops). Note that approximate BrO plume locations are indicated by red dashed boxes in Fig. 7. Cloud tops indicate boundaries regarding vertical mixing. Hence, it is likely that vertical transport of tropospheric bromine from the ground was also limited to 3 km height along CALIPSO footprints. However, the maximum time difference between CALIOP and GOME-2 observations is about 1.5 h so that cloud and aerosol conditions shown in Fig. 7 may differ in the vertical from the one at GOME-2 observation time.

FLEXPART simulations from FS1 for the mature and dissolving stage of the BCTE are displayed by Fig. 8 together with corresponding GOME-2 observations of tropospheric BrO VCD for reference. For 1 April, the best agreement between FLEXPART and GOME-2 is achieved by assuming that the BrO plume was located within a 1 km thick layer at the surface at time of initialisation (1 April at 00:00 UTC). The magnitude of BrO observations within the plume is reproduced well by FLEXPART. The model under-

A bromine explosion event linked to cyclone development in the Arctic

A.-M. Blechschmidt et al.

Title Page

Abstract

Introduction

Conclusions

References

Tables

Figures



Back

Close

Full Screen / Esc

Printer-friendly Version

Interactive Discussion



A bromine explosion event linked to cyclone development in the Arctic

A.-M. Blechschmidt et al.

Title Page

Abstract

Introduction

Conclusions

References

Tables

Figures



Back

Close

Full Screen / Esc

Printer-friendly Version

Interactive Discussion



9–11 km. FS2 runs predict large values of tropospheric BrO vertical column density in the same area as the satellite observations, but also further northwards of the satellite observed plume. FS2 overestimates the magnitude of values reached inside the plume. In contrast to FS1 and FS2, FS3 results agree well with satellite observations at the dissolving stage of the BCTE. The simulated plume has largely lost its comma-shape for FS3. The best agreement between satellite retrievals and FS3 runs is achieved when assuming that the plume was located between 0 and 1 km altitude at time of initialisation (2 April 00:00 UTC). The fact that FS3 results compare much better with satellite data than FS2 and FS1 shows that emission sources around -150° E, 75° N contributed to the long observed lifetime (about four days) of the BrO plume. WRF simulations show that high wind speeds, convergent air flow and hence uplift occurred in this region (see above). This, together with SMOS and MODIS images suggests that recycling of bromine on salty blowing snow most likely caused the long observed lifetime of the BCTE.

Overall, FLEXPART runs show that the plume was located in the troposphere with largest concentrations close to the surface, confirming that GOME-2 observed a tropospheric feature. Further investigation of FLEXPART runs shows that the plume resided between 0 and 3 km altitude during the whole simulation time. Provided that cloud top heights are representative of the upper limit of convection, FLEXPART simulations agree well with cloud top heights observed by CALIOP, further indicating that the BrO plume most likely occurred in the lowest three kilometres of the troposphere.

5 Summary and conclusions

An intense BCTE which developed on 31 March 2011 over the Beaufort Sea has been investigated based on combined use of satellite observations and numerical models. Despite the short atmospheric lifetime of BrO, the high wind speed BCTE was observed for about four days in GOME-2 satellite images. Comparison of GOME-2 satellite retrievals to FLEXPART and WRF model results reveals that the BrO plume moved

source regions for salty blowing snow production observed by SMOS. Results presented in this paper document that weather conditions associated with fronts within polar cyclones are favorable not only for development of BEEs, but also to sustain high values of tropospheric BrO, thereby extending plume lifetime substantially.

GOME-2 satellite observations of tropospheric BrO and total column ozone together with MODIS false colour images show, that the plume was spatially separated from the dry conveyor belt associated with the polar cyclone. In this sense, this BEE differs from previous case studies for which the dry conveyor belt as a potentially bromine-rich stratospheric airstream complicated the interpretation of tropospheric BrO or total column BrO from satellite retrievals (e.g., Begoin et al., 2010; Salawitch et al., 2010). Moreover, FLEXPART simulations suggest that the BrO plume developed in a 1 km thick layer near the surface and was then transported up to 3 km altitude. This combination of model results and satellite observations shows that the BrO plume observed by GOME-2 most likely resided in the lowest parts of the troposphere over the entire lifetime of the BCTE. Our findings are consistent with Jones et al. (2010) who found that ozone depletion events which extend above 1 km in the vertical are usually associated with high wind speed conditions. Our results demonstrate that the close proximity of fronts and dry conveyor belts needs to be considered when deciding whether cyclone-like shaped plumes observed from satellite are of tropospheric or stratospheric origin, as both would be expected to show a comma- or spiral-shaped BrO pattern. This issue can be solved by using meteorological model data in combination with satellite observations.

The BrO plume occurred at the same location as low level clouds observed by MODIS and CALIOP. As described in Sect. 2.1, light path enhancement and shielding of boundary layer BrO from the satellite sensors view cannot account for the plume pattern observed by GOME-2. Assuming that clouds are representative of vertical boundaries regarding convection, cloud and aerosol top heights observed by CALIOP agree well with FLEXPART results indicating that plume transport was limited to the lowest 3 km of the atmosphere.

A bromine explosion event linked to cyclone development in the Arctic

A.-M. Blechschmidt et al.

Title Page	
Abstract	Introduction
Conclusions	References
Tables	Figures
◀	▶
◀	▶
Back	Close
Full Screen / Esc	
Printer-friendly Version	
Interactive Discussion	



for providing model source code on their webpages (<http://www2.mmm.ucar.edu/wrf/users/> and <https://flexpart.eu/>, respectively).

The article processing charges for this open-access publication
5 were covered by the University of Bremen.

References

Afe, O. T., Richter, A., Sierk, B., Wittrock, F., and Burrows, J. P.: BrO emission from volcanoes: a survey using GOME and SCIAMACHY measurements, *Geophys. Res. Lett.*, 31, L24113, doi:10.1029/2004GL020994, 2004. 24961

10 Barrie, L. and Platt, U.: Arctic tropospheric chemistry: an overview, *Tellus B*, 49, 450–454, 1997. 24957

Barrie, L. A., Bottenheim, J. W., Schnell, R. C., Crutzen, P. J., and Rasmussen, R. A.: Ozone destruction and photochemical reactions at polar sunrise in the lower Arctic atmosphere, *Nature*, 334, 138–141, 1988. 24957, 24959

15 Begoin, M., Richter, A., Weber, M., Kaleschke, L., Tian-Kunze, X., Stohl, A., Theys, N., and Burrows, J. P.: Satellite observations of long range transport of a large BrO plume in the Arctic, *Atmos. Chem. Phys.*, 10, 6515–6526, doi:10.5194/acp-10-6515-2010, 2010. 24960, 24961, 24962, 24965, 24966, 24970, 24974, 24975

20 Bottenheim, J. W., Netcheva, S., Morin, S., and Nghiem, S. V.: Ozone in the boundary layer air over the Arctic Ocean: measurements during the TARA transpolar drift 2006–2008, *Atmos. Chem. Phys.*, 9, 4545–4557, doi:10.5194/acp-9-4545-2009, 2009. 24959

Bracher, A., Lamsal, L. N., Weber, M., Bramstedt, K., Coldewey-Egbers, M., and Burrows, J. P.: Global satellite validation of SCIAMACHY O₃ columns with GOME WFDOAS, *Atmos. Chem. Phys.*, 5, 2357–2368, doi:10.5194/acp-5-2357-2005, 2005. 24963

25 Browning, K. A.: The dry intrusion perspective of extra-tropical cyclone development, *Meteorol. Appl.*, 4, 317–324, 1997. 24970

Burrows, J. P., Dehn, A., Deters, B., Himmelmann, S., Richter, A., Voigt, S., and Orphal, J.: Atmospheric remote-sensing reference data from GOME: Part 1. Temperature-dependent absorption cross-sections of NO₂ in the 231–794 nm range, *J. Quant. Spectrosc. Ra.*, 60, 1025–1031, 1998. 24961

A bromine explosion event linked to cyclone development in the Arctic

A.-M. Blechschmidt et al.

Title Page

Abstract

Introduction

Conclusions

References

Tables

Figures



Back

Close

Full Screen / Esc

Printer-friendly Version

Interactive Discussion

- Buyts, Z., Brough, N., Huey, L. G., Tanner, D. J., von Glasow, R., and Jones, A. E.: High temporal resolution Br₂, BrCl and BrO observations in coastal Antarctica, *Atmos. Chem. Phys.*, 13, 1329–1343, doi:10.5194/acp-13-1329-2013, 2013. 24957
- Callies, J., Corpaccioli, E., Eisinger, M., Hahne, A., and Lefebvre, A.: GOME-2 – Metop's second-generation sensor for operational ozone monitoring, *ESA Bull-Eur. Space*, 102, 28–36, 2000. 24961
- Choi, S., Wang, Y., Salawitch, R. J., Canty, T., Joiner, J., Zeng, T., Kurosu, T. P., Chance, K., Richter, A., Huey, L. G., Liao, J., Neuman, J. A., Nowak, J. B., Dibb, J. E., Weinheimer, A. J., Diskin, G., Ryerson, T. B., da Silva, A., Curry, J., Kinnison, D., Tilmes, S., and Lev-elt, P. F.: Analysis of satellite-derived Arctic tropospheric BrO columns in conjunction with aircraft measurements during ARCTAS and ARCPAC, *Atmos. Chem. Phys.*, 12, 1255–1285, doi:10.5194/acp-12-1255-2012, 2012. 24956
- Coldewey-Egbers, M., Weber, M., Lamsal, L. N., de Beek, R., Buchwitz, M., and Burrows, J. P.: Total ozone retrieval from GOME UV spectral data using the weighting function DOAS approach, *Atmos. Chem. Phys.*, 5, 1015–1025, doi:10.5194/acp-5-1015-2005, 2005. 24963
- Domine, F., Taillandier, A. S., Simpson, W. R., and Severin, K.: Specific surface area, density and microstructure of frost flowers, *Geophys. Res. Lett.*, 32, L13502, doi:10.1029/2005GL023245, 2005. 24958
- Dudhia, J.: Numerical study of convection observed during the Winter Monsoon Experiment using a mesoscale two-dimensional model, *J. Atmos. Sci.*, 46, 3077–3107, 1989. 24965
- Errera, Q., Daerden, F., Chabrilat, S., Lambert, J. C., Lahoz, W. A., Viscardy, S., Bonjean, S., and Fonteyn, D.: 4D-Var assimilation of MIPAS chemical observations: ozone and nitrogen dioxide analyses, *Atmos. Chem. Phys.*, 8, 6169–6187, doi:10.5194/acp-8-6169-2008, 2008. 24961
- Fickert, S., Adams, J. W., and Crowley, J. N.: Activation of Br₂ and BrCl via uptake of HOBr onto aqueous salt solutions, *J. Geophys. Res.*, 104, 23719–23727, doi:10.1029/1999JD900359, 1999. 24957
- Fleischmann, O. C., Hartmann, M., Burrows, J. P., and Orphal, J.: New ultraviolet absorption cross-sections of BrO at atmospheric temperatures measured by time-windowing Fourier transform spectroscopy, *J. Photochem. Photobio. A*, 168, 117–132, doi:10.1016/j.jphotochem.2004.03.026, 2004. 24961

A bromine explosion event linked to cyclone development in the Arctic

A.-M. Blechschmidt et al.

Title Page

Abstract

Introduction

Conclusions

References

Tables

Figures



Back

Close

Full Screen / Esc

Printer-friendly Version

Interactive Discussion



Frieß, U., Hollwedel, J., König-Langlo, G., Wagner, T., and Platt, U.: Dynamics and chemistry of tropospheric bromine explosion events in the Antarctic coastal region, *J. Geophys. Res.*, 109, D06305, doi:10.1029/2003JD004133, 2004.

Frieß, U., Sihler, H., Sander, R., Pöhler, D., Yilmaz, S., and Platt, U.: The vertical distribution of BrO and aerosols in the Arctic: measurements by active and passive differential optical absorption spectroscopy, *J. Geophys. Res.*, 116, D00R04, doi:10.1029/2011JD015938, 2011.

Gilman, J. B., Burkhardt, J. F., Lerner, B. M., Williams, E. J., Kuster, W. C., Goldan, P. D., Murphy, P. C., Warneke, C., Fowler, C., Montzka, S. A., Miller, B. R., Miller, L., Oltmans, S. J., Ryerson, T. B., Cooper, O. R., Stohl, A., and de Gouw, J. A.: Ozone variability and halogen oxidation within the Arctic and sub-Arctic springtime boundary layer, *Atmos. Chem. Phys.*, 10, 10223–10236, doi:10.5194/acp-10-10223-2010, 2010. 24965

Gorshelev, V., Serdyuchenko, A., Weber, M., Chehade, W., and Burrows, J. P.: High spectral resolution ozone absorption cross-sections – Part 1: Measurements, data analysis and comparison with previous measurements around 293 K, *Atmos. Meas. Tech.*, 7, 609–624, doi:10.5194/amt-7-609-2014, 2014. 24961

Grell, G. A., Peckham, S. E., Schmitz, R., McKeen, S. A., Frost, G., Skamarock, W. C., and Eder, B.: Fully coupled online chemistry within the WRF model, *Atmos. Environ.*, 39, 6957–6976, doi:10.1016/j.atmosenv.2005.04.027, 2005. 24976

Hirdman, D., Burkhardt, J. F., Sodemann, H., Eckhardt, S., Jefferson, A., Quinn, P. K., Sharma, S., Ström, J., and Stohl, A.: Long-term trends of black carbon and sulphate aerosol in the Arctic: changes in atmospheric transport and source region emissions, *Atmos. Chem. Phys.*, 10, 9351–9368, doi:10.5194/acp-10-9351-2010, 2010. 24965

Hollwedel, J., Wenig, M., Beirle, S., Kraus, S., Köhl, S., Wilms-Grabe, W., Platt, U., and Wagner, T.: Year-to-Year Variations of Polar Tropospheric BrO as seen by GOME, *Adv. Space Res.*, 34, 804–808, doi:10.1016/j.asr.2003.08.060, 2004. 24956

Jacobi, H.-W., Morin, S., and Bottenheim, J. W.: Observation of widespread depletion of ozone in the springtime boundary layer of the central Arctic linked to mesoscale synoptic conditions, *J. Geophys. Res.*, 115, D17302, doi:10.1029/2010JD013940, 2010. 24959

Janjic, Z. I.: The step-mountain eta coordinate model: further developments of the convection, viscous sublayer, and turbulence closure schemes, *Mon. Weather Rev.*, 122, 927–945, 1994. 24965

Jones, A. E., Anderson, P. S., Begoin, M., Brough, N., Hutterli, M. A., Marshall, G. J., Richter, A., Roscoe, H. K., and Wolff, E. W.: BrO, blizzards, and drivers of polar tropospheric ozone

A bromine explosion event linked to cyclone development in the Arctic

A.-M. Blechschmidt et al.

[Title Page](#)[Abstract](#)[Introduction](#)[Conclusions](#)[References](#)[Tables](#)[Figures](#)[Back](#)[Close](#)[Full Screen / Esc](#)[Printer-friendly Version](#)[Interactive Discussion](#)

depletion events, *Atmos. Chem. Phys.*, 9, 4639–4652, doi:10.5194/acp-9-4639-2009, 2009. 24957, 24959, 24960, 24970, 24974

Jones, A. E., Anderson, P. S., Wolff, E. W., Roscoe, H. K., Marshall, G. J., Richter, A., Brough, N., and Colwell, S. R.: Vertical structure of Antarctic tropospheric ozone depletion events: characteristics and broader implications, *Atmos. Chem. Phys.*, 10, 7775–7794, doi:10.5194/acp-10-7775-2010, 2010. 24960, 24975

Jones, A. E., Wolff, E. W., Brough, N., Bauguitte, S. J.-B., Weller, R., Yela, M., Navarro-Comas, M., Ochoa, H. A., and Theys, N.: The spatial scale of ozone depletion events derived from an autonomous surface ozone network in coastal Antarctica, *Atmos. Chem. Phys.*, 13, 1457–1467, doi:10.5194/acp-13-1457-2013, 2013. 24957

Kaleschke, L., Richter, A., Burrows, J. P., Afe, O., Heygster, G., Notholt, J., Rankin, A. M., Roscoe, H. K., Hollwedel, J., Wagner, T., and Jacobi, H.-W.: Frost flowers on sea ice as a source of sea salt and their influence on tropospheric halogen chemistry, *Geophys. Res. Lett.*, 31, L16114, doi:10.1029/2004GL020655, 2004. 24957

Kaleschke, L., Tian-Kunze, X., Maaß, N., Mäkynen, M., and Drusch, M.: Sea ice thickness retrieval from SMOS brightness temperatures during the Arctic freeze-up period, *Geophys. Res. Lett.*, 39, L05501, doi:10.1029/2012GL050916, 2012.

Kalnay, E., Kanamitsu, M., Kistler, R., Collins, W., Deaven, D., Gandin, L., Iredell, M., Saha, S., White, G., Woollen, J., Zhu, Y., Leetmaa, A., Reynolds, R., Chelliah, M., Ebisuzaki, W., Higgins, W., Janowiak, J., Mo, K. C., Ropelewski, C., Wang, J., Jenne, R., and Joseph, D.: The NCEP/NCAR 40 Year Reanalysis Project, *B. Am. Meteorol. Soc.*, 77, 437–471, doi:10.1175/1520-0477(1996)077<0437:tnyrp>2.0.co;2, 1996. 24968

Koo, J.-H., Wang, Y., Kurosu, T. P., Chance, K., Rozanov, A., Richter, A., Oltmans, S. J., Thompson, A. M., Hair, J. W., Fenn, M. A., Weinheimer, A. J., Ryerson, T. B., Solberg, S., Huey, L. G., Liao, J., Dibb, J. E., Neuman, J. A., Nowak, J. B., Pierce, R. B., Natarajan, M., and Al-Saadi, J.: Characteristics of tropospheric ozone depletion events in the Arctic spring: analysis of the ARCTAS, ARCPAC, and ARCIONS measurements and satellite BrO observations, *Atmos. Chem. Phys.*, 12, 9909–9922, doi:10.5194/acp-12-9909-2012, 2012. 24959

Lehrer, E., Wagenbach, D., and Platt, U.: Aerosol chemical composition during tropospheric ozone depletion at Ny Alesund/Svalbard, *Tellus B*, 49, 486–495, 1997. 24957

Lin, Y.-L., Farley, R. D., and Orville, H. D.: Bulk parameterization of the snow field in a cloud model, *J. Clim. Appl. Meteorol.*, 22, 1065–1092, 1983. 24965

A bromine explosion event linked to cyclone development in the Arctic

A.-M. Blechschmidt et al.

[Title Page](#)[Abstract](#)[Introduction](#)[Conclusions](#)[References](#)[Tables](#)[Figures](#)[Back](#)[Close](#)[Full Screen / Esc](#)[Printer-friendly Version](#)[Interactive Discussion](#)

Rozanov, A., Rozanov, V., Buchwitz, M., Kokhanovsky, A., and Burrows, J. P.: SCIATRAN 2.0 – a new radiative transfer model for geophysical applications in the 175–2400 nm spectral region, *Adv. Space Res.*, 36, 1015–1019, doi:10.1016/j.asr.2005.03.012, 2005. 24962

Salawitch, R. J., Canty, T., Kurosu, T., Chance, K., Liang, Q., da Silva, A., Pawson, S., Nielsen, J. E., Rodriguez, J. M., Bhartia, P. K., Liu, X., Huey, L. G., Liao, J., Stickel, R. E., Tanner, D. J., Dibb, J. E., Simpson, W. R., Donohoue, D., Weinheimer, A. J., Flocke, F., Knapp, D., Montzka, D. D., Neuman, J. A., Nowak, J. B., Ryerson, T. B., Oltmans, S., Blake, D. R., Atlas, E. L., Kinnison, D. E., Tilmes, S., Pan, L. L., Hendrick, F., Van Roozendael, M., Kreher, K., Johnston, P. V., Gao, R. S., Johnson, B., Bui, T. P., Chen, G., Pierce, R. B., Crawford, J. H., and Jacob, D. J.: A New interpretation of total column BrO during Arctic spring, *Geophys. Res. Lett.*, 37, L21805, doi:10.1029/2010GL043798, 2010. 24957, 24970, 24975

Sander, R., Burrows, J., and Kaleschke, L.: Carbonate precipitation in brine – a potential trigger for tropospheric ozone depletion events, *Atmos. Chem. Phys.*, 6, 4653–4658, doi:10.5194/acp-6-4653-2006, 2006. 24957, 24958, 24959, 24969, 24974

Serdyuchenko, A., Gorshelev, V., Weber, M., Chehade, W., and Burrows, J. P.: High spectral resolution ozone absorption cross-sections – Part 2: Temperature dependence, *Atmos. Meas. Tech.*, 7, 625–636, doi:10.5194/amt-7-625-2014, 2014. 24961

Sihler, H., Platt, U., Beirle, S., Marbach, T., Kühl, S., Dörner, S., Verschaeve, J., Frieß, U., Pöhler, D., Vogel, L., Sander, R., and Wagner, T.: Tropospheric BrO column densities in the Arctic derived from satellite: retrieval and comparison to ground-based measurements, *Atmos. Meas. Tech.*, 5, 2779–2807, doi:10.5194/amt-5-2779-2012, 2012. 24956, 24962

Sihler, H., Dörner, S., Pozzer, A., Frieß, U., Platt, U., and Wagner, T.: Meteorology and vertical structure of plumes of enhanced bromine monoxide as detected by satellite remote sensing during Arctic spring, *EGU General Assembly, Vienna, Austria, 27 April–2 May 2014, EGU2014-15426*, 2014. 24974

Simpson, W. R., Carlson, D., Hönninger, G., Douglas, T. A., Sturm, M., Perovich, D., and Platt, U.: First-year sea-ice contact predicts bromine monoxide (BrO) levels at Barrow, Alaska better than potential frost flower contact, *Atmos. Chem. Phys.*, 7, 621–627, doi:10.5194/acp-7-621-2007, 2007a. 24958

Simpson, W. R., von Glasow, R., Riedel, K., Anderson, P., Ariya, P., Bottenheim, J., Burrows, J., Carpenter, L. J., Frieß, U., Goodsite, M. E., Heard, D., Hutterli, M., Jacobi, H.-W., Kaleschke, L., Neff, B., Plane, J., Platt, U., Richter, A., Roscoe, H., Sander, R., Shepson, P., Sodeau, J., Steffen, A., Wagner, T., and Wolff, E.: Halogens and their role in polar boundary-

A bromine explosion event linked to cyclone development in the Arctic

A.-M. Blechschmidt et al.

[Title Page](#)[Abstract](#)[Introduction](#)[Conclusions](#)[References](#)[Tables](#)[Figures](#)[Back](#)[Close](#)[Full Screen / Esc](#)[Printer-friendly Version](#)[Interactive Discussion](#)

layer ozone depletion, *Atmos. Chem. Phys.*, 7, 4375–4418, doi:10.5194/acp-7-4375-2007, 2007b. 24957, 24959

Skamarock, W. C., Klemp, J. B., Dudhia, J., Gill, D. O., Barker, D. M., Duda, M., Huang, X.-Y., Wang, W., and Powers, J. G.: A Description of the Advanced Research WRF Version 3, NCAR Technical note NCAR/TN-475+STR, doi:10.5065/D68S4MVH, NCAR, Boulder (Colorado), 2008. 24960, 24965

Steffen, A., Douglas, T., Amyot, M., Ariya, P., Aspmo, K., Berg, T., Bottenheim, J., Brooks, S., Cobbett, F., Dastoor, A., Dommergue, A., Ebinghaus, R., Ferrari, C., Gardfeldt, K., Goodsite, M. E., Lean, D., Poulain, A. J., Scherz, C., Skov, H., Sommar, J., and Temme, C.: A synthesis of atmospheric mercury depletion event chemistry in the atmosphere and snow, *Atmos. Chem. Phys.*, 8, 1445–1482, doi:10.5194/acp-8-1445-2008, 2008. 24959

Stohl, A.: Characteristics of atmospheric transport into the Arctic troposphere, *J. Geophys. Res.*, 111, D11306, doi:10.1029/2005JD006888, 2006. 24965

Stohl, A., Forster, C., Frank, A., Seibert, P., and Wotawa, G.: Technical note: The Lagrangian particle dispersion model FLEXPART version 6.2, *Atmos. Chem. Phys.*, 5, 2461–2474, doi:10.5194/acp-5-2461-2005, 2005. 24960, 24965

Tarasick, D. W. and Bottenheim, J. W.: Surface ozone depletion episodes in the Arctic and Antarctic from historical ozonesonde records, *Atmos. Chem. Phys.*, 2, 197–205, doi:10.5194/acp-2-197-2002, 2002. 24959

Theys, N., Van Roozendaal, M., Hendrick, F., Yang, X., De Smedt, I., Richter, A., Begoin, M., Errera, Q., Johnston, P. V., Kreher, K., and De Mazière, M.: Global observations of tropospheric BrO columns using GOME-2 satellite data, *Atmos. Chem. Phys.*, 11, 1791–1811, doi:10.5194/acp-11-1791-2011, 2011. 24956, 24961

Vavrus, S. J.: Extreme Arctic cyclones in CMIP5 historical simulations, *Geophys. Res. Lett.*, 40, 6208–6212, doi:10.1002/2013GL058161, 2013. 24976

Viscardy, S., Errera, Q., Christophe, Y., Chabrilat, S., and Lambert, J.-C.: Evaluation of ozone analysis from UARS MLS assimilation by BASCOE between 1992 and 1997, *JSTARS*, 3, 190–202, 2010. 24961

Vogt, R., Crutzen, P. J., and Sander, R.: A mechanism for halogen release from sea-salt aerosol in the remote marine boundary layer, *Nature*, 383, 327–330, doi:10.1038/383327A0, 1996.

Vountas, M., Rozanov, V. V., and Burrows, J. P.: Ring-effect: impact of rotational raman scattering on radiative transfer in earth's atmosphere, *J. Quant. Spectrosc. Ra.*, 60, 943–961, doi:10.1016/S0022-4073(97)00186-6, 1998. 24961

- Wagner, T. and Platt, U.: Satellite mapping of enhanced BrO concentrations in the troposphere, *Nature*, 395, 486–490, 1998. 24956
- Wagner, T., Leue, C., Wenig, M., Pfeilsticker, K., and Platt, U.: Spatial and temporal distribution of enhanced boundary layer BrO concentrations measured by the GOME instrument aboard ERS-2, *J. Geophys. Res.*, 106, 24225–24235, doi:10.1029/2000JD000201, 2001. 24958
- 5 Warneke, C., Bahreini, R., Brioude, J., Brock, C. A., de Gouw, J. A., Fahey, D. W., Froyd, K. D., Holloway, J. S., Middlebrook, A., Miller, L., Montzka, S., Murphy, D. M., Peischl, J., Ryonson, T. B., Schwarz, J. P., Spackman, J. R., and Veres, P.: Biomass burning in Siberia and Kazakhstan as an important source for haze over the Alaskan Arctic in April 2008, *Geophys. Res. Lett.*, 36, L02813, doi:10.1029/2008GL036194, 2009. 24965
- 10 Weber, M., Lamsal, L. N., Coldewey-Egbers, M., Bramstedt, K., and Burrows, J. P.: Pole-to-pole validation of GOME WFDOAS total ozone with groundbased data, *Atmos. Chem. Phys.*, 5, 1341–1355, doi:10.5194/acp-5-1341-2005, 2005. 24963
- 15 Yang, X., Pyle, J. A., Cox, R. A., Theys, N., and Van Roozendaal, M.: Snow-sourced bromine and its implications for polar tropospheric ozone, *Atmos. Chem. Phys.*, 10, 7763–7773, doi:10.5194/acp-10-7763-2010, 2010. 24958, 24976
- Zhao, X., Strong, K., Adams, C., Schofield, R., Yang, X., Richter, A., Friess, U., Blechschmidt, A.-M., and Koo, J.-H.: A case study of a transported bromine explosion event in the Canadian High Arctic, *J. Geophys. Res.*, in review, 2015. 24969, 24974

A bromine explosion event linked to cyclone development in the Arctic

A.-M. Blechschmidt et al.

[Title Page](#)[Abstract](#)[Introduction](#)[Conclusions](#)[References](#)[Tables](#)[Figures](#)[Back](#)[Close](#)[Full Screen / Esc](#)[Printer-friendly Version](#)[Interactive Discussion](#)

A bromine explosion event linked to cyclone development in the Arctic

A.-M. Blechschmidt et al.

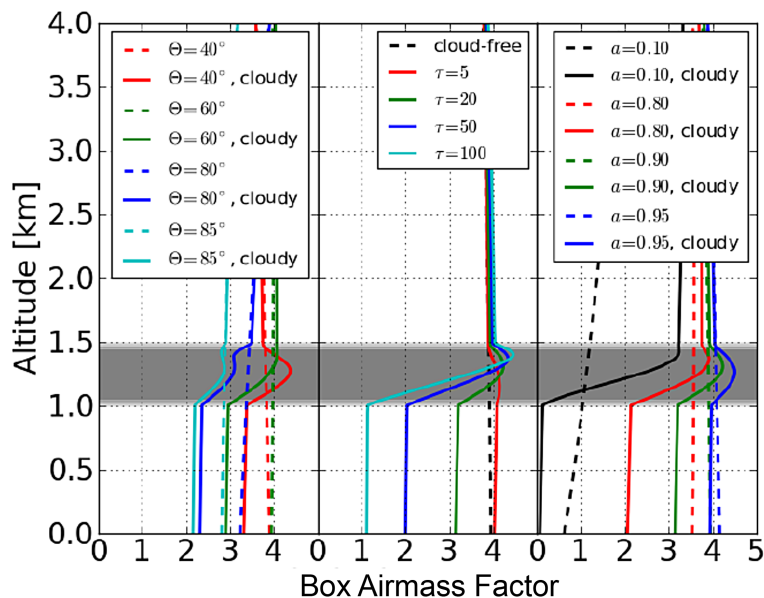


Figure 1. Radiative transfer simulations showing sensitivity of satellite observations to BrO in the boundary layer under (dashed lines) cloud free and (solid lines) cloudy conditions. The panels show the influence of (left) solar zenith angle θ , (middle) cloud optical thickness τ and (right) surface albedo a on the box airmass factor. All simulations are at a wavelength of 350 nm, $\theta = 50^\circ$, $\tau = 20$, and $a = 0.9$ unless noted otherwise.

[Title Page](#)
[Abstract](#)
[Introduction](#)
[Conclusions](#)
[References](#)
[Tables](#)
[Figures](#)
[Back](#)
[Close](#)
[Full Screen / Esc](#)
[Printer-friendly Version](#)
[Interactive Discussion](#)

A bromine explosion event linked to cyclone development in the Arctic

A.-M. Blechschmidt et al.

Title Page

Abstract

Introduction

Conclusions

References

Tables

Figures



Back

Close

Full Screen / Esc

Printer-friendly Version

Interactive Discussion

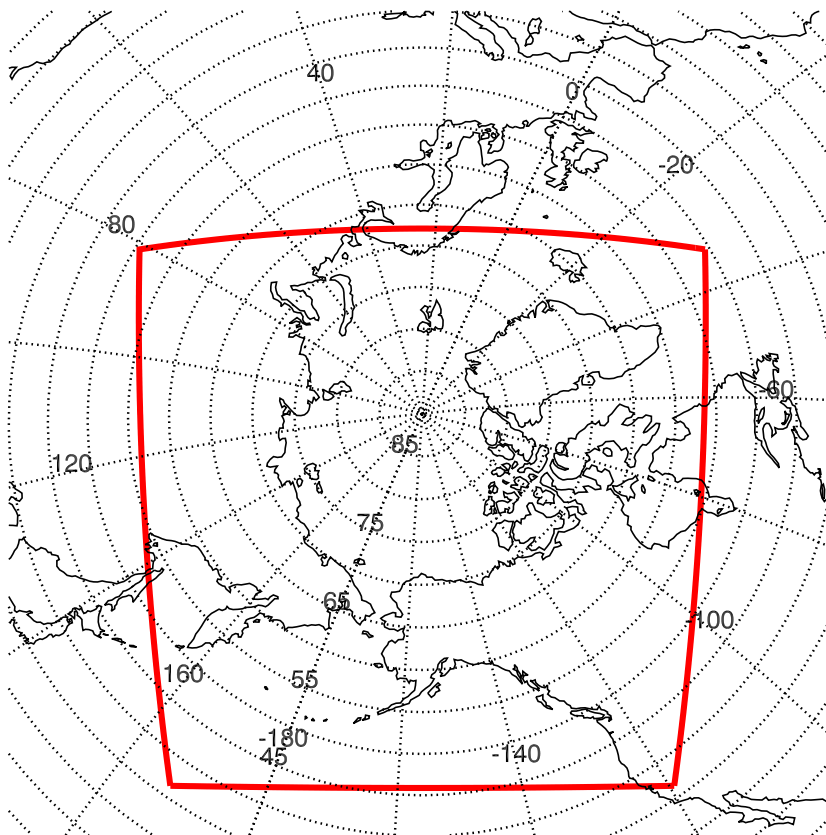


Figure 2. The WRF model domain (red box).

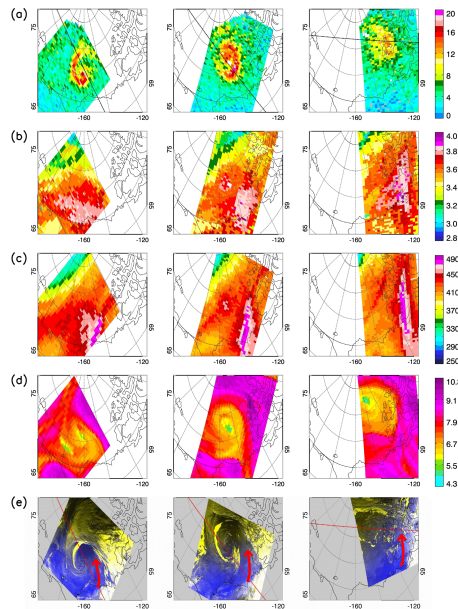


Figure 3. Satellite observations, together with parameters used for GOME-2 tropospheric BrO retrieval, of the BCTE showing **(a)** GOME-2 BrO tropospheric VCD [10^{13} molec cm^{-2}], **(b)** GOME-2 BrO stratospheric VCD [10^{13} molec cm^{-2}], **(c)** GOME-2 ozone VCD [DU], **(d)** WRF tropopause height [km] and **(e)** MODIS false colour images. Shown from left to right are different development stages of the BCTE: onset (31 March 2011 at 23:30 UTC for GOME-2 and WRF, 23:15 UTC for MODIS), mature stage (1 April 2011 at 21:30 UTC for GOME-2 and WRF, 22:20 UTC for MODIS) and dissolving stage (2 April 2011 at 19:30 UTC for GOME-2 and WRF, 19:45 UTC for MODIS). Red arrows plotted on top of MODIS false colour images indicate the location of the dry conveyor belt (see Sect. 4 for further details). The red dotted lines in MODIS false colour images and black dotted lines in GOME-2 BrO tropospheric VCD images correspond to CALIPSO tracks for the CALIOP observations shown in Fig. 7.

A bromine explosion event linked to cyclone development in the Arctic

A.-M. Blechschmidt et al.

Title Page

Abstract

Introduction

Conclusions

References

Tables

Figures



Back

Close

Full Screen / Esc

Printer-friendly Version

Interactive Discussion



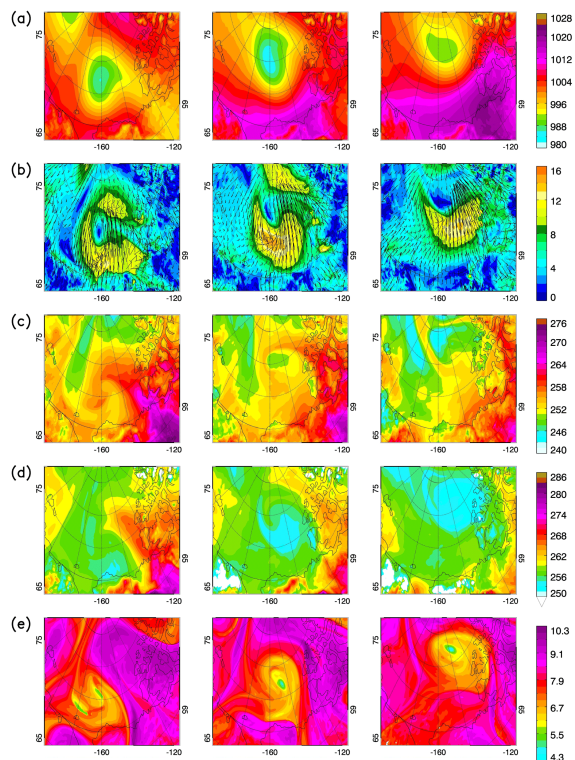


Figure 4. WRF weather simulations of the BCTE for **(a)** sea level pressure [hPa], **(b)** wind direction (black arrows) and wind speed [m s^{-1}] (coloured shadings), **(c)** temperature [K] at 2 m above ground and **(d)** temperature [K] at 350 gpm (note that the colourbar differs for **(c, d)**). Shown from left to right are simulations for different development stages of the BCTE: onset (31 March 2011 at 23:30 UTC), mature stage (1 April 2011 at 21:30 UTC) and dissolving stage (2 April 2011 at 19:30 UTC).

A bromine explosion event linked to cyclone development in the Arctic

A.-M. Blechschmidt et al.

Title Page

Abstract

Introduction

Conclusions

References

Tables

Figures



Back

Close

Full Screen / Esc

Printer-friendly Version

Interactive Discussion



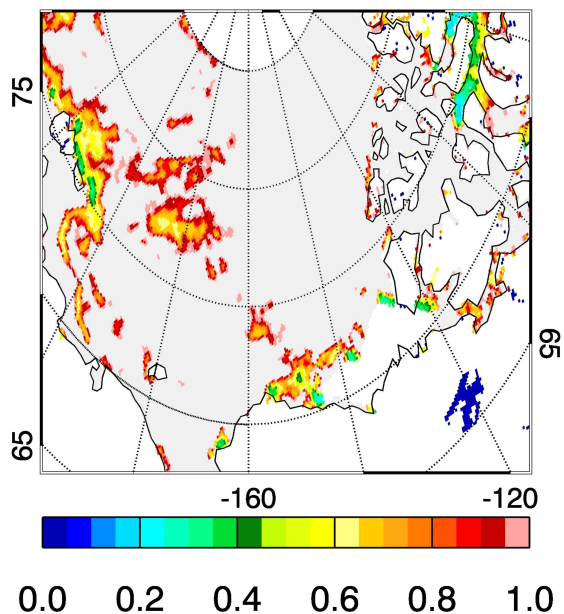


Figure 5. SMOS satellite retrievals of sea ice thickness [m] for 1 April 2011. Values larger than 1 m are generally related to large uncertainties and are therefore shown in light grey colour.

A bromine explosion event linked to cyclone development in the Arctic

A.-M. Blechschmidt et al.

Title Page

Abstract Introduction

Conclusions References

Tables Figures

◀ ▶

◀ ▶

Back Close

Full Screen / Esc

Printer-friendly Version

Interactive Discussion



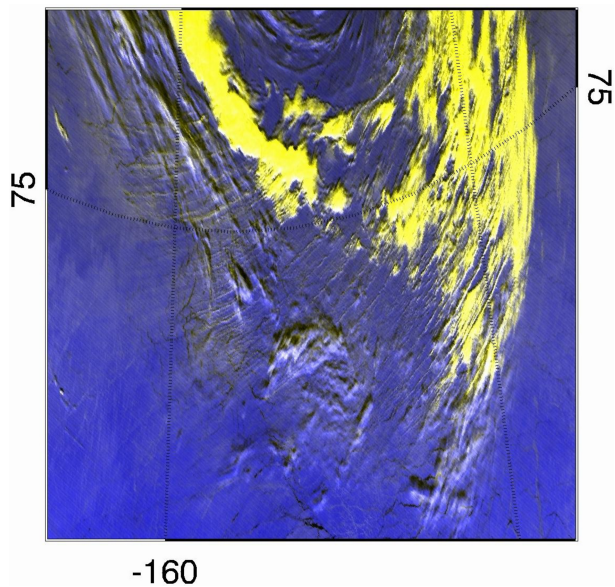


Figure 6. MODIS false colour image for 1 April 2011 at 22:20 UTC. Shown is a subarea of the MODIS image given in the middle panel of Fig. 3e. Snow and ice on the ground should appear blue, while clouds and suspended snow particles should appear yellow (see Sect. 2.2).

A bromine explosion event linked to cyclone development in the Arctic

A.-M. Blechschmidt et al.

Title Page

Abstract Introduction

Conclusions References

Tables Figures

◀ ▶

◀ ▶

Back Close

Full Screen / Esc

Printer-friendly Version

Interactive Discussion



A bromine explosion event linked to cyclone development in the Arctic

A.-M. Blechschmidt et al.

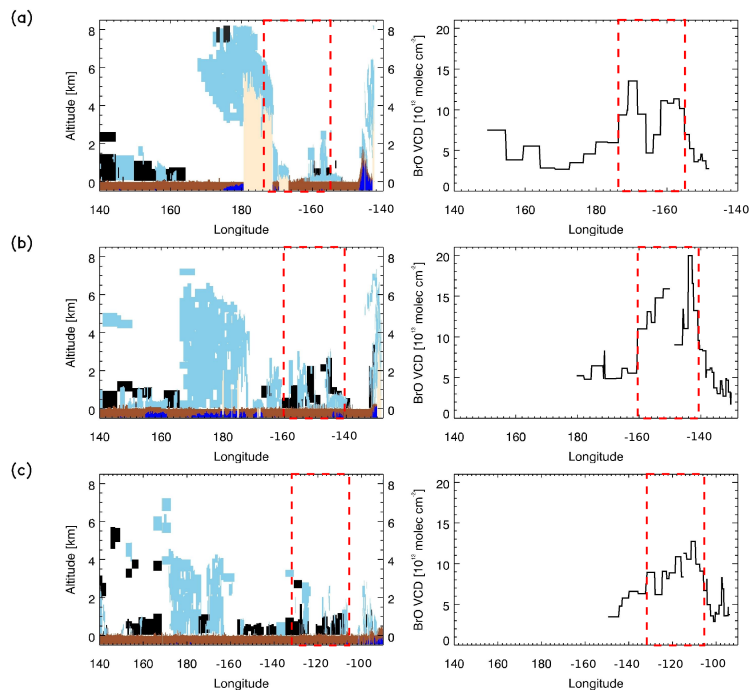


Figure 7. Satellite observations of the BCTE showing CALIOP vertical feature mask (white – clear air, light blue – cloud, black – aerosol, beige – no signal, brown – surface, dark blue – subsurface) on the left and GOME-2 BrO tropospheric VCD [10^{13} molec cm^{-2}] along the CALIPSO tracks on the right. Corresponding CALIPSO tracks are plotted on top of GOME-2 BrO tropospheric VCD and MODIS false colour images in Fig. 3 (a, e), respectively. Shown are observations for different development stages of the BCTE: **(a)** onset (31 March 2011 at 21:17 UTC for CALIOP, 23:30 UTC for GOME-2), **(b)** mature stage (1 April 2011 at 20:21 UTC for CALIOP, 21:30 UTC for GOME-2) and **(c)** dissolving stage (2 April 2011 at 17:47 UTC for CALIOP, 19:30 UTC for GOME-2). The red dashed boxes indicate approximate locations of the BrO plume. Longitudes on x axes are given in degrees West.

[Title Page](#)
[Abstract](#)
[Introduction](#)
[Conclusions](#)
[References](#)
[Tables](#)
[Figures](#)
[Back](#)
[Close](#)
[Full Screen / Esc](#)
[Printer-friendly Version](#)
[Interactive Discussion](#)

A bromine explosion event linked to cyclone development in the Arctic

A.-M. Blechschmidt et al.

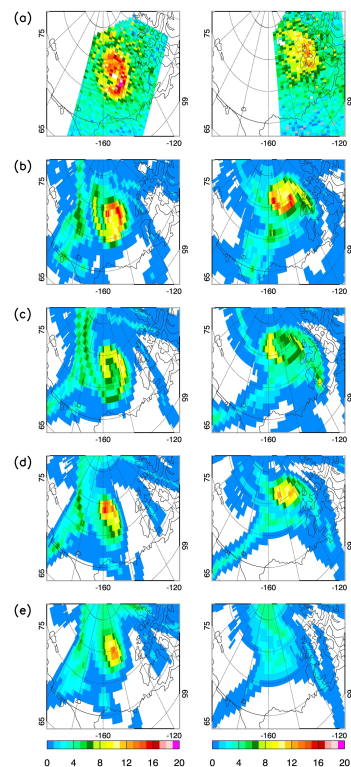


Figure 8. FLEXPART FS1 simulations of BrO tropospheric VCD [10^{13} molec cm^{-2}] for (left) 1 April 2011 at 21:30 UTC (mature stage of the BCTE) and (right) 2 April 2011 at 19:30 UTC (dissolving stage of the BCTE) assuming that the plume was located between **(b)** 0–1 km, **(c)** 3–5 km, **(d)** 7–9 km and **(e)** 9–11 km altitude at time of initialisation. The corresponding GOME-2 retrievals of BrO tropospheric VCD [10^{13} molec cm^{-2}] are shown by panels in **(a)** for comparison. See Sect. 3.2 for details on the model set-up.

[Title Page](#)
[Abstract](#)
[Introduction](#)
[Conclusions](#)
[References](#)
[Tables](#)
[Figures](#)
[Back](#)
[Close](#)
[Full Screen / Esc](#)
[Printer-friendly Version](#)
[Interactive Discussion](#)

A bromine explosion event linked to cyclone development in the Arctic

A.-M. Blechschmidt et al.

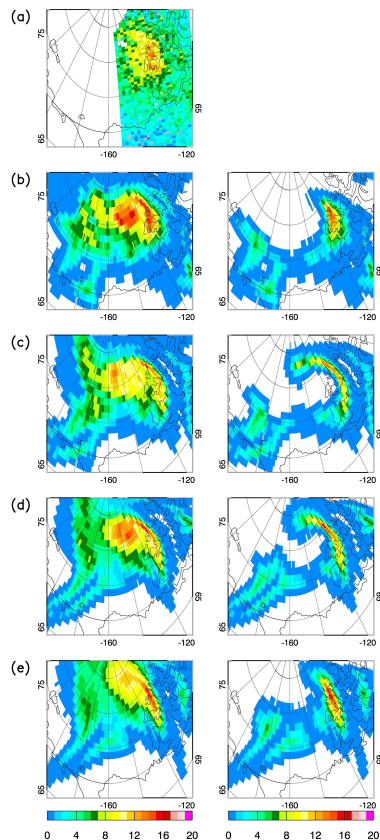


Figure 9. As in Fig. 8 but for FLEXPART (left) FS2 and (right) FS3 simulations for 2 April 2011 at 19:30 UTC (dissolving stage of the BCTE).

[Title Page](#)[Abstract](#)[Introduction](#)[Conclusions](#)[References](#)[Tables](#)[Figures](#)[Back](#)[Close](#)[Full Screen / Esc](#)[Printer-friendly Version](#)[Interactive Discussion](#)